Sonochemical oxidation of piroxicam drug: Effect of key operating parameters and degradation pathways

Sonochemical oxidation of piroxicam drug: Effect of key operating parameters and degradation pathways

Athina Lianou,[a] Zacharias Frontistis,[a*] Efthalia Chatzisymeon,[b] Maria Antonopoulou,[c] Ioannis Konstantinou,[d] and Dionissios Mantzavinos[a]

(a) Department of Chemical Engineering, University of Patras, Caratheodory 1, University Campus, GR-26504 Patras, Greece

(b) Institute for Infrastructure and Environment, School of Engineering, The University of Edinburgh, Edinburgh EH9 3JL, United Kingdom

(c) Department of Environmental & Natural Resources Management, University of Patras, 2 Seferi St., GR-30100 Agrinio, Greece

(d) Department of Chemistry, University of Ioannina, GR-45110 Ioannina, Greece

* Corresponding author:

Email: zfrontistis@chemeng.upatras.gr; Tel.: +302610996137; Fax: +302610969532

Abstract

BACKGROUND: Piroxicam (PRX) is a non-steroidal anti-inflammatory drug (NSAID) commonly used to relieve pain and swelling of conditions like arthritis. PRX has been extensively detected in seawater, surface, and sewage waters worldwide and therefore its efficient treatment is an issue of emerging concern. In this work, the sonochemical degradation of PRX was investigated.

RESULTS: All experiments were conducted at constant ultrasound frequency of 20 kHz while the following range of experimental conditions was investigated: initial PRX concentration 320–960μg/L, ultrasound power density 20–60 W/L, temperature 20–60 ^{o}C, reaction time up to 60 min. The effect of different water matrices, namely surface water (SW), bottled water (BW), ultrapure water (UPW) and humic acid (HA) aqueous solution on process efficiency was also explored. It was found that PRX degradation reached 96% after only 10 min of treatment at the best conditions (i.e. $[PRX]_0$=320 mg/L, 20^{o}C, 36 W/L) assayed. Power density could positively affect PRX degradation. Nevertheless, PRX degradation decreased when its initial concentration and the temperature of the bulk liquid was increased. PRX degradation was found to decrease, in different water matrices, in the order: UPW > 5 mg/L HA > BW > 10 mg/L HA >SW. High resolution mass spectrometry analysis revealed that fourteen transformation by-products (TBPs) were formed and subsequently degraded during treatment while the PRX degradation pathways were also elucidated.

CONCLUSION: At the optimal operating conditions assayed, PRX was efficiently degraded after about 10 min of sonochemical oxidation, thus rendering it a promising technology for the treatment of xenobiotics

Keywords: NSAIDs; wastewater treatment; ultrasound; pharmaceuticals; intermediate products

1. Introduction

Piroxicam (PRX) is a non-steroidal anti-inflammatory drug (NSAID) commonly used to relieve pain and swelling of conditions like arthritis. NSAIDs, including PRX, have been extensively detected in seawater, surface, and sewage waters worldwide,[1-3] since these are among the most frequently used drugs (painkillers, antipyretics, treatment of inflammations and prevention of myocardial infarction). The presence of such drugs, even at low concentrations (from ng/L to mg/L), can have a significant impact on the aquatic and terrestrial systems, and therefore this is an issue of emerging concern.[4]

Excretion (from human and animal medical care) is the major source of water and soil pollution by drugs. These are excreted as unchanged or metabolites, which after disposal to municipal sewage systems find their way to the environment.[3] Wastewater treatment plants (WWTPs) have been mainly designed to remove suspended solids and organic content while their effect on the removal of micropollutants may be, in most cases, negligible.[1] Therefore, when drugs enter conventional biological WWTPs, only a small fraction is removed and residual amounts are released into the terrestrial and aquatic environment, causing major environmental and health concerns. Due to inadequacy of current WWTPs to completely remove such contaminants, additional or alternative processes should be applied to support existing treatment facilities and increase their efficiency.

Sonochemical oxidation is an advanced oxidation process (AOP), which has gained considerable attention over the past decades for the treatment of several trace pollutants, including pharmaceutical substances.[5-7] Sonochemical oxidation is based on the in situ generation of powerful oxidizing agents, such as the hydroxyl radical. These are formed through the cyclic formation, growth and implosive collapse of bubbles that behave as hot-spot, micro-reactors.[8,9] At

sufficient contact time and proper operating conditions, sonochemical oxidation may mineralize all organic carbon to CO_2, which is the most stable end product of chemical oxidation. The sonochemical degradation of various NSAIDs, such as ibuprofen,[10,11] naproxen,[12] and diclofenac[13-16] has been investigated. Nevertheless, to the best of our knowledge, there is no study on the sonochemical degradation of PRX, a commonly used NSAID. In addition, unlike other drugs, the advanced oxidation of PRX has been merely explored. Specifically, there is only one study by Feng et al.,[17] who investigated the degradation of three NSAIDs, including PRX by means of ozone or H_2O_2/O_3 treatment. That study focused on determining the bio-availability of chemical intermediates formed in ozonated water onto a biofilm-supporting granular activated carbon.

The purpose of this work is to investigate the sonochemical oxidation of PRX, evaluate the effect of key operating parameters that can determine degradation rates and propose degradation pathways. Therefore, the following parameters, namely initial PRX concentration, power density, reaction time, water matrix, and temperature are studied. Transformation by-products are identified and a potential degradation pathway is proposed.

2. Materials and methods

2.1 Materials

Piroxicam (PRX) ($C_{15}H_{13}N_3O_4S$, CAS no: 36322-90-4) was supplied by Sigma–Aldrich and used as received. All experiments, unless otherwise stated, were performed in ultrapure water (UPW) with pH = 6.5 taken from a water purification system (EASYpureRF-Barnstead/Thermolyne, USA). Two more water matrices were employed for this study. One was a commercially available bottled water (BW) (pH = 7.5, 0.4 mS/cm conductivity containing 211 mg/L bicarbonate, 10 mg/L

chloride, 15 mg/L sulfate, 5 mg/L nitrate and 78 mg/L of various metal ions), and the other was surface water (SW) collected from a stream near the city of Athens, Greece (pH=7.8, 166 mg/L bicarbonate, 11 mg/ chloride, and 51 mg/L sulfate). Humic acid (HA, CAS number 1415-93-6) was purchased from Sigma–Aldrich. Sodium chloride (NaCl, CAS no: 7647-14-5) and sodium bicarbonate ($NaHCO_3$, CAS no: 144-55-8), used as free radical scavengers, were purchased from Sigma-Aldrich.

2.2 Ultrasound irradiation

A Branson 450 horn-type digital sonifier operating at a fixed frequency of 20 kHz and a variable power output up to 450W (nominal) was employed. Sonochemical oxidation took place in a cylindrical, double-walled, Pyrex vessel, which was open to the atmosphere. Ultrasound irradiation was emitted through a 1 cm in diameter titanium tip which was positioned in the middle of the vessel at a distance of 3 cm from the bottom. The working volume was 0.12 L and the actual power density emitted to the bulk solution was determined calorimetrically and it was found to be between 20 and 60 W/L. Temperature was kept at 20 ^{o}C, unless otherwise stated, by a temperature control unit. Most experiments were performed in duplicate and mean values, whose standard deviation never exceeded 5%. Samples of 1.2 mL were periodically taken from the reactor and analyzed as follows.

2.3 Chromatographic techniques

High performance liquid chromatography (HPLC: Alliance 2695, Waters) was employed to monitor the concentration of PRX. Separation was achieved on a Kinetex XB-C18 100A column

(2.6 μm, 2.1 mm × 150 mm) and a 0.5 μm inline filter (KrudKatcher Ultra) both purchased from Phenomenex. The mobile phase consisting of 68:32 water:acetonitrile eluted isocratically at 0.35 mL/min and 45 ºC, while the injection volume was 100 μL. Detection was achieved through a photodiode array detector (Waters 2996 PDA detector, detection λ = 350 nm). The limit of detection was 3.52 μg/L, and the limit of quantitation was 11.75 μg/L

LC-MS/TOF analysis was carried out on a system, consisted of a Dionex UHPLC Ultimate 3000 connected to a BRUKER micrOTOF Focus II mass spectrometer. Gradient methods were developed on a Thermo Scientific Acclaim ^{TM} RSLC 120 C18 column (protected by a guard from Waters) thermostated at 30° C, using a mixture of water/1mM ammonium formate and methanol as mobile phase at a flow rate of 0.3 mL/min. The elution starts with 1% methanol and progressively increases to 99% (methanol) at 10 min. At 12 min the initial conditions are reached and retained for 3 min (15 min). The micrOTOF Focus II was operated in both ionization modes (positive and negative) as follows: dry gas at 8 L/min, nebulizer press at 2.4 bar, dry heater at 200° C, hexapole RF at 100 Vpp and capillary voltage at 4500 V. Accurate mass measurements provided by micrOTOF Focus II mass spectrometer and the interpretation of fragments derived from in source Collision-induced Dissociation (isCID) was used for the structural assignment of transformation by-products (TBPs).

3. Results and discussion

3.1 Effect of initial PRX concentration

The effect of initial PRX concentration, ranging from 320 μg/L to 960 μg/L, on its degradation rate was studied. Figure 1 shows PRX degradation as a function of treatment time at 36 W/L power

density, and constant temperature of 20 °C. Complete removal is achieved after 25 min of treatment for 640–960 μg/L PRX and this decreases to almost 10 min when initial PRX concentration is 320 μg/L. Data of Figure 1 are found to fit well a pseudo first-order reaction, which is in agreement with previous studies on sonochemical degradation of other NSAIDs, such as ibuprofen [18] and diclofenac [14,15,19]. In the inset graph of Figure 1 it is observed that the kinetic rate coefficients, k, decrease when the initial substrate concentration is increased. For example, rate coefficients are 0.1459 min^{-1}, 0.1695 min^{-1} and 0.2098 min^{-1} when the initial PRX concentration is 960 μg/L, 640 μg/L and 320 μg/L, respectively. The fact that rate coefficient changes with varying PRX concentration implies that the reaction is not true first order although data fitting to first-order kinetics equation (i.e. Ln $[PRX]_o/[PRX]=kt$) is good.

Figure 1.

3.2 Effect of power density

Ultrasound power is a key operating parameter that can substantially affect efficiency of sonochemical oxidation. Therefore, different power densities, ranging from 20 to 60 W/L, were applied for the degradation of 640 μg/L PRX and the results are shown in Figure 2. As seen conversion increases with increasing applied power. Not only this but, as shown in the inset graph of Figure 2, a nearly linear increase of PRX degradation with power density is observed. Specifically, reaction rate coefficients are 0.1157 min^{-1} (r^2=0.9688), 0.1695 min^{-1} (r^2=0.9868) and 0.1967 min^{-1} (r^2=0.9921) when power density is 20, 36 and 60 W/L, respectively. This increase of PRX degradation can be attributed to the fact that, at higher power levels, the transmittance of

ultrasonic energy into the reactor increases. As a result, a larger number of cavitation bubbles are formed and the pulsation and collapse of bubbles occur at a faster rate, thus increasing significantly the concentration of hydroxyl radicals generated, and the subsequent H_2O_2 production in the liquid mixture, leading to enhanced organics degradation rates.[20-22] Furthermore, an increase in ultrasonic power contributes to higher mixing intensity due to the turbulence and microstreaming which are generated during the cavitational microbubble collapse,[23] which can also contribute to increased PRX degradation rates.

Figure 2.

3.3 Effect of bulk temperature

Experiments were performed at 20 ºC, 40 ºC and 60 ºC in order to study the effect of temperature on the degradation of 320 μg/L PRX at 36 W/L power density. Results in Figure 3 show that an increase in bulk temperature can reduce process efficiency, and therefore total degradation of PRX is achieved after about 10, 20 and 40 min of sonochemical treatment at 20 ºC, 40 ºC and 60 ºC, respectively. Temperature of the bulk liquid can affect several parameters such as the vapor pressure, viscosity, gas solubility and surface tension. Therefore, the negative effect of temperature on PRX degradation may be explained by the following: the increase in temperature increases the vapor pressure of the solvent. Consequently, the cavitation bubbles contain more water vapor. Because of this increased vapor content, the collapse of the cavitation bubbles is less violent, which is known as the 'cushioning effect'. This causes a reduction in the collapse temperature and thus a reduced production of ˙OH radicals. In addition to this, increased temperatures are likely to favour

degassing of the liquid phase, thus reducing the number of gas nuclei available for bubble formation.[20,24]

Figure 3.

3.4 Effect of the water matrix

The complexity of the water matrix is another operating parameter that can affect process efficiency. To assess its effect, experiments were conducted in surface water (SW), bottled water (BW), as well as in UPW spiked with humic acid (HA) at two concentrations (5 and 10 mg/L); in all cases, PRX concentration was 320 μg/L and the power density 36 W/L at 20 ^{o}C. Results in Figure 4 show that there is a decrease in the degradation rate in the presence of HA, BW and SW compared to that of UPW. This may be attributed to the fact that HA, BW, and SW contain other organic or inorganic substances that can act as hydroxyl radical scavengers and can therefore significantly lower the degradation of the target contaminant[25]. Specifically, PRX degradation is found to decrease in the order: UPW (0.2098 min^{-1}) > 5 mg/L HA (0.1005 min^{-1}) > BW (0.0819 min^{-1}) > 10 mg/L HA (0.0706 min^{-1}) > SW (0.0646 min^{-1}) with numbers in brackets corresponding to kinetic rate coefficient. The lower degradation rates in the presence of HA, a model natural organic matter (NOM), may be due to the much higher concentration of organic carbon in the solution (5–10 mg/L HA versus 320 μg/L PRX), which competes with the substrate for the oxidative species[26]. Moreover, it is observed that increase of the initial HA concentration, from 5 to 10 mg/L, negatively affects PRX degradation, since the amount of the organics competing with PRX is higher at 10 mg/L than at 5 mg/L HA. PRX degradation in SW, which is the most complex

matrix studied, since it consists of NOM and several inorganic substances, is found to be lower than in all other water matrices. Therefore, results indicate that when the complexity of the water matrix is increased process efficiency is decreased.

Figure 4.

The presence of chlorides and bicarbonates in BW and SW partially impedes degradation since inorganics can scavenge hydroxyl radicals[26]. This was further demonstrated by performing experiments in UPW spiked with chlorides, in the form of NaCl, and sodium bicarbonate for degrading 320 μg/L PRX at 36 W/L power density and 20 ºC. As shown in Figure 5, PRX degradation rate is substantially decreased in the presence of 250-500 mg/L NaCl as well as of 50-250 mg/L BIC. Results from this work are in agreement with previous studies dealing with the sonochemical degradation of drugs. For example, Xiao et al.[11] found that in the presence of terephthalate (TA), a typical •OH scavenger and dissolved Suwannee river fulvic acid (SRFA) the degradation rates of ciprofloxacin and ibuprofen are significantly reduced compared to no TA or SRFA present. Moreover, Gao et al. [22] reported that sulfamethoxazole degradation was inhibited in the presence of NO_3^{-1}, Cl^- and SO_4^{-2} and the inhibition degree followed the order of NO_3^{-1},> Cl^- > SO_4^{-2}.

Figure 5.

3.5 Identification of transformation by-products (TBPs) and degradation pathways

Simultaneously with PRX degradation, the formation and subsequent degradation of 14 TBPs was revealed. Structural assignment was based on high resolution accurate mass measurements in both positive and negative ionization mode (Tables 1 and 2). Firstly, under negative ionization mode PRX presents a molecular ion peak [M-H]- at m/z 330.0554 and fragments (isCID MS) at m/z 266.0922 and 210.0224, which correspond to the loss of $-SO_2$ followed intramolecular rearrangement and loss of pyridinecarboxamide moiety, respectively. The fragment ion at m/z 146.0602 is generated by the loss of $-SO_2$ followed intramolecular rearrangement from the 210.0224 fragment ion. Three TBPs (TBP 9, 10, 12) with molecular ions at m/z 346.0493-346.0506 that differ about 16 amu from the PRX are identified as hydroxylated derivatives. Pyridine, benzothiazine moieties and N-methyl group can be considered as potential sites of hydroxylation. TBP 12 shows a fragment at m/z 226.0180 which corresponds to the loss of pyridinecarboxamide moiety indicating that hydroxylation takes place at the benzothiazine moiety or N-methyl group. On the other hand, TBP 9 and 10 show close retention times but no diagnostic fragments. However, the hydroxylation of PRX molecule in the pyridinyl ring and more specifically at the 5'-position can be proposed for one of the isomeric TBPs since 5'-hydroxypiroxicam is reported as a well-known metabolite of PRX in the literature.[28]

In addition, two di-hydroxylated TBPs (TBP 6 and 11) are detected on the basis of +32 amu difference from the PRX molecule. TBP 11 shows a characteristic diagnostic fragment at m/z 210.0224 corresponding to the loss of $C_6H_4N_2O_3$ suggesting that hydroxylation takes place on the pyridinyl ring. Four isomeric TBPs (TBP 4, 5, 7, 8) with m/z 212.0015-212.0030 and TBP 3 are proposed as the mono- and di-hydroxylatedbenzothiazine derivatives, respectively. Finally, TBPs 1, 2, 13 and 14 are identified as 1,2-benzisothiazol-3(2H)-one-1,1-dioxide, N-methyl-

benzenesulfonamide, N1-(pyridin-2-yl)oxalamide and N1-methyl-N2-(pyridin-2-yl)oxalamide. The profiles (peak area vs irradiation time) of the TBPs are shown in Figure 6. The sequence of the PRX transformation paths can be proposed based on the time within the maximum concentration of each TBP is observed. Therefore, TBPs 9, 10 and 12 (mono-hydroxy-TBPs) peaked up at 120 min allows us to consider them as first-stages TBPs. Di-hydroxylated-PRX derivatives (TBPs 6 and 11) and mono-, di-hydroxylated benzothiazine derivatives (TBPs 4, 5, 7 and 8) peaked up at 180 min can be considered as secondary products. Finally, TBPs 1, 2, 13 and 14 are detected only in samples after 240 min of treatment and at low concentration levels and thus they can be considered as later stage products. For the sake of comparison with other studies dealing with the degradation of PRX, TBP 14 and structurally similar TBPs have been also identified as degradation products of PRX under oxidative and photolytic conditions.[29-32] In addition, the in vivo formation of the metabolic oxidation product 5-hydroxypiroxicam and at least 13 new secondary peaks (without structure identification) after the in vitro study of hydroxyl radical attack of PRX was reported elsewhere.[33]

Taking into account the identification and structural assignment of the TBPs, as well as their evolution profiles, the sonochemical degradation mechanisms of PRX are proposed in Figure 7. The first steps of degradation start with hydroxyl radical attack on PRX molecule leading to the formation of hydroxylated, di-hydroxylated derivatives. In parallel, apart from the generation and attack of hydroxyl radicals, singlet oxygen ($^1O_2$) can be also formed in ample amounts [34] during the ultrasound treatment. PRX quenches $^1O_2$ with rate constants in the order of 10^8 M^{-1} s^{-1} showing a significant photodegradation efficiency, as reported elsewhere.[35] This pathway proceeds by the addition of singlet oxygen to the enol double bond and the formation of a dioxetane intermediate. Ring cleavage of this unstable intermediate, leads to its conversion in a carboxylic acid structure,

as depicted in Figure 7 [29,30,32], which is further transformed to later stages TBPs, such as TBP 1, 2, 13 and 14. The same degradation mechanism was proposed for the photochemical oxidation of PRX.[29,30,32]

4. Conclusions

The aim of this work was to investigate the sonochemical degradation of piroxicam (PRX), a commonly used non-steroidal anti-inflammatory drug. For this purpose, the effect of key operating parameters was evaluated. The following parameters, namely initial PRX concentration, ultrasound power density, temperature, water matrix, and treatment time were studied. Transformation by-products were identified and a potential degradation pathway was identified. The main findings drawn from this study are summarized below.

- An increase of power density leads to enhanced PRX degradation rates, since at high power densities the amount of hydroxyl radicals generated and the mixing intensity are increased.
- Increasing the temperature of the bulk liquid results in a reduction of sonochemical activity and this may be attributed to the 'cushioning' phenomenon.
- Water matrices containing organic and inorganic radical scavengers can have adverse effect on degradation kinetics compared to runs in ultrapure water. Also, when the complexity of the water matrix is increased process efficiency is decreased.
- Sonochemical degradation starts with hydroxyl radical attacking on PRX molecule leading to the formation of hydroxylated and di-hydroxylated derivatives. At the same time, singlet oxygen is added to the enol double bond, thus leading to the formation of a dioxetane

intermediate, which is consequently converted to a carboxylic acid structure and other later stages transformation by-products.

In general ultrasound irradiation seems a promising technology with relative high efficiency (i.e removal of hundreds of μg/L in less than few minutes) for the destruction of micro pollutants. Further research is needed with particular emphasis at the scale up of the process in order to study the industrial application of sonochemsitry in environmental protection.

References

1. Lolić A, Paíga P, Santos LHMLM, Ramos S, Correia M and Delerue-Matos C, Assessment of non-steroidal anti-inflammatory and analgesic pharmaceuticals in seawaters of North of Portugal: Occurrence and environmental risk. *Sci Total Environ* **508**: 240–250 (2015).

2. Mainero Rocca L, Gentili A, Caretti F, Curini R and Pérez-Fernández V, Occurrence of non-steroidal anti-inflammatory drugs in surface waters of Central Italy by liquid chromatography–tandem mass spectrometry. *Int J Environ Anal Chem* **95**: 685–697 (2015).

3. Ziylan A and Ince NH, The occurrence and fate of anti-inflammatory and analgesic pharmaceuticals in sewage and fresh water: Treatability by conventional and non-conventional processes. *J Hazard Mater* **187**: 24–36 (2011).

4. Bácsi I, B-Béres V, Kókai Z, Gonda S, Novák Z, Nagy SA and Vasas G, Effects of non-steroidal anti-inflammatory drugs on cyanobacteria and algae in laboratory strains and in natural algal assemblages. *Environ Pollut* **212**: 508–518 (2016).

5. Tran N, Drogui P and Brar SK, Sonochemical techniques to degrade pharmaceutical organic pollutants. *Environ Chem Lett* **13**: 251–268 (2015).

6. Tran N, Drogui P and Brar SK, Sonoelectrochemical oxidation of carbamazepine in waters: optimization using response surface methodology. *J Chem Technol Biotechnol* **90**: 921–929 (2015).

7. Ma X, Tang K, Li Q, Song Y, Ni Y and Gao N, Parameters on 17β-Estradiol degradation by Ultrasound in an aqueous system. *J Chem Technol Biotechnol* **89**: 322–327 (2014).

8. Darsinou B, Frontistis Z, Antonopoulou M, Konstantinou I and Mantzavinos D, Sono-activated persulfate oxidation of bisphenol A: Kinetics, pathways and the controversial role of temperature. *Chem Eng J* **280**: 623–633 (2015).

9. Oztekin R and Sponza DT, Treatment of wastewaters from the olive mill industry by sonication. *J Chem Technol Biotechnol* **88**: 212–225 (2013).

10. Méndez-Arriaga F, Torres-Palma RA, Pétrier C, Esplugas S, Gimenez J and Pulgarin C, Ultrasonic treatment of water contaminated with ibuprofen. *Water Res* **42**: 4243–4248 (2008).

11. Xiao R, He Z, Diaz-Rivera D, Pee GY and Weavers LK, Sonochemical degradation of ciprofloxacin and ibuprofen in the presence of matrix organic compounds. *Ultrason Sonochem* **21**: 428–435 (2014).

12. Im J-K, Heo J, Boateng LK, Her N, Flora JRV, Yoon J, Zoh KD and Yoon Y, Ultrasonic degradation of acetaminophen and naproxen in the presence of single-walled carbon nanotubes. *J Hazard Mater* **254**: 284–292 (2013).

13. Ziylan A, Koltypin Y, Gedanken A and Ince NH, More on sonolytic and sonocatalytic decomposition of Diclofenac using zero-valent iron. *Ultrason Sonochem* **20**: 580–586 (2013).

14. Güyer GT and Ince NH, Degradation of diclofenac in water by homogeneous and heterogeneous sonolysis. *Ultrason Sonochem* **18**: 114–119 (2011).

15. Naddeo V, Landi M, Scannapieco D and Belgiorno V, Sonochemical degradation of twenty-three emerging contaminants in urban wastewater. *Desalin Water Treat* **51**: 6601–6608 (2013).

16. Naddeo V, Belgiorno V, Kassinos D, Mantzavinos D and Meric S, Ultrasonic degradation, mineralization and detoxification of diclofenac in water: Optimization of operating parameters. *Ultrason Sonochem* **17**: 179–185 (2010).

17. Feng L, Watts MJ, Yeh D, Esposito G and van Hullebusch ED, The Efficacy of Ozone/BAC Treatment on Non-Steroidal Anti-Inflammatory Drug Removal from Drinking Water and Surface Water. *Ozone Sci Eng* **37**: 343–356 (2015).

18. Madhavan J, Grieser F and Ashokkumar M, Combined advanced oxidation processes for the synergistic degradation of ibuprofen in aqueous environments. *J Hazard Mater* **178**: 202–208 (2010).

19. Madhavan J, Kumar PSS, Anandan S, Zhou M, Grieser F and Ashokkumar M, Ultrasound assisted photocatalytic degradation of diclofenac in an aqueous environment. *Chemosphere* **80**: 747–752 (2010).

20. Psillakis E, Mantzavinos D and Kalogerakis N, Monitoring the sonochemical degradation of phthalate esters in water using solid-phase microextraction. *Chemosphere* **54**: 849–857 (2004).

21. Torres RA, Pétrier C, Combet E, Carrier M and Pulgarin C, Ultrasonic cavitation applied to the treatment of bisphenol A. Effect of sonochemical parameters and analysis of BPA by-products. *Ultrason Sonochem* **15**: 605–611 (2008).

22. Gao Y, Gao N, Deng Y, Gu J, Gu Y and Zhang D, Factors affecting sonolytic degradation of sulfamethazine in water. *Ultrason Sonochem* **20**: 1401–1407 (2013).

23. Mowla A, Mehrvar M and Dhib R, Combination of sonophotolysis and aerobic activated sludge processes for treatment of synthetic pharmaceutical wastewater. *Chem Eng J* **255**: 411–423 (2014).

24. Emery RJ, Papadaki M, Freitas dos Santos LM and Mantzavinos D, Extent of sonochemical degradation and change of toxicity of a pharmaceutical precursor (triphenylphosphine oxide) in water as a function of treatment conditions. *Environ Int* **31**: 207–211 (2005).

25. Gogate R, Mujumdar S, Pandit A, Sonochemical reactors for waste water treatment: comparison using formic acid degradation as a model reaction *Adv Environ Res* **7**:283-299 (2003).

26. Rayaroth M, Aravind U, Aravindakumar T, Sonochemical degradation of Coomassie Brilliant Blue: Effect of frequency, power density, pH and various additives. *Chemocsphere* **119**: 848-855 (2015).

27. Guzman-Duque F, Petrier C, Pulgarin C, Penueal G, Torres-Palma R, Effects of sonochemical parameters and inorganic ions during the sonochemical degradation of crystal violet in water. *Ultrason Sonochem* **18**:440-446 (2011).

28. McKinney AR, Suann CJ and Stenhouse AM, The detection of piroxicam, tenoxicam and their metabolites in equine urine by electrospray ionisation ion trap mass spectrometry. *Rapid Commun Mass Spectrom* **18**: 2338–2342 (2004).

29. Glass BD, Brown ME, Daya S, Worthington MS, Drummond P, Antunes E, Lebete M, Anoopkumar-Dukie M and Maharaj D, Influence of cyclodextrins on the photostability of selected drug molecules in solution and the solid-state. *Int J Photoenergy* **3**: 205–211 (2001).

30. Modhave DT, Handa T, Shah RP and Singh S, Successful characterization of degradation products of drugs using LC-MS tools: Application to piroxicam and meloxicam. *Anal Methods* **3**: 2864 (2011).

31. Tománková H and Šabartová J, Determination of potential degradation products of piroxicam by HPTLC densiometry and HPLC. *Chromatographia* **28**: 197–202 (1989).

32. Ilic-Stojanovic S, Nikolic V, Nikolic L, Zdravkovic A, Kapor A, Popsavin M and Petrovic D, The improved photostability of naproxen in the inclusion complex with 2-hydroxypropyl-β-cyclodextrin. *Hem Ind* **69**: 361–370 (2015).

33. Gaudiano M., Valvo L, Bertocchi P and Manna L, RP-HPLC study of the degradation of diclofenac and piroxicam in the presence of hydroxyl radicals. *J Pharm Biomed Anal* **32**: 151–158 (2003).

34. Matsumura Y, Iwasawa A, Kobayashi T, Kamachi T, Ozawa T and Kohno M, Detection of High-frequency Ultrasound-induced Singlet Oxygen by the ESR Spin-trapping Method *Chem Lett* **42**: 1291–1293 (2013).

35. Ferrari G V., Natera J, Paulina Montaña M, Muñoz V, Gutiérrez EL, Massad W, Miskoski S and Garcia NA, Scavenging of photogenerated ROS by Oxicams. Possible biological and environmental implications. *J Photochem Photobiol B Biol* **153**: 233–239 (2015).

List of Tables

402 **Table 1.**

TBP code	R_t (min)	Deprotonated molecular formula	m/z $[M-H]^-$	Δ (ppm)	RDBE
TBP1	4.4	$C_7H_4NO_3S$	181.9925	-4.0	6.5
TBP2	4.7	$C_7H_8NO_2S$	170.0276	3.2	4.5
TBP3	5.1	$C_8H_6NO_5S$	227.9972	-1.2	6.5
TBP4	5.4	$C_8H_6NO_4S$	212.0030	-3.4	6.5
TBP5	6.0	$C_8H_6NO_4S$	212.0021	0.9	6.5
TBP6*	6.1	$C_{15}H_{12}N_3O_6S$	362.0452	0	11.5
TBP7	6.3	$C_8H_6NO_4S$	212.0026	-1.2	6.5
TBP8	6.6	$C_8H_6NO_4S$	212.0015	4.0	6.5
TBP9*	6.9	$C_{15}H_{12}N_3O_5S$	346.0493	3.0	11.5
		$C_{15}H_{12}N_3O_3$	282.0875	3.3	11.5
TBP10*	7.1	$C_{15}H_{12}N_3O_5S$	346.0494	2.7	11.5
		$C_{15}H_{12}N_3O_3$	282.0875	3.3	11.5
PRX	7.2	$C_{15}H_{12}N_3O_4S$	330.0554	0	11.5
		$C_{15}H_{12}N_3O_2$	266.0922	4.9	11.5
		$C_9H_8NO_3S$	210.0224	2.9	6.5
		C_9H_8NO	146.0602	6.6	6.5
TBP11*	7.6	$C_{15}H_{12}N_3O_6S$	362.0450	0.7	11.5
		$C_{15}H_{12}N_3O_2$	266.0922	4.9	11.5
		$C_9H_8NO_3S$	210.0224	2.9	6.5
		C_9H_8NO	146.0602	6.6	6.5
TBP12*	8.0	$C_{15}H_{12}N_3O_5S$	346.0506	-0.8	11.5
		$C_9H_8NO_4S$	226.0180	-1.4	6.5

403

404 **Table 2.**

TBP code	R_t (min)	Protonated molecular formula	m/z $[M+H]^+$	Δ (ppm)	RDBE
TBP13	5.8	$C_7H_8N_3O_2$	166.0615	-2.4	5.5
TBP14	6.4	$C_8H_{10}N_3O_2$	180.0775	-3.9	5.5
TBP6*	6.1	$C_{15}H_{14}N_3O_6S$	364.0591	1.9	10.5
TBP9*	6.9	$C_{15}H_{14}N_3O_5S$	348.0650	-0.3	10.5
TBP10*	7.1	$C_{15}H_{14}N_3O_5S$	348.0651	-0.7	10.5
PRX	7.2	$C_{15}H_{14}N_3O_4S$	332.0687	3.9	10.5
TBP11*	7.6	$C_{15}H_{14}N_3O_6S$	364.0595	0.8	10.5
TBP12*	8.0	$C_{15}H_{14}N_3O_5S$	348.0650	-0.3	10.5

405

406

List of Figures

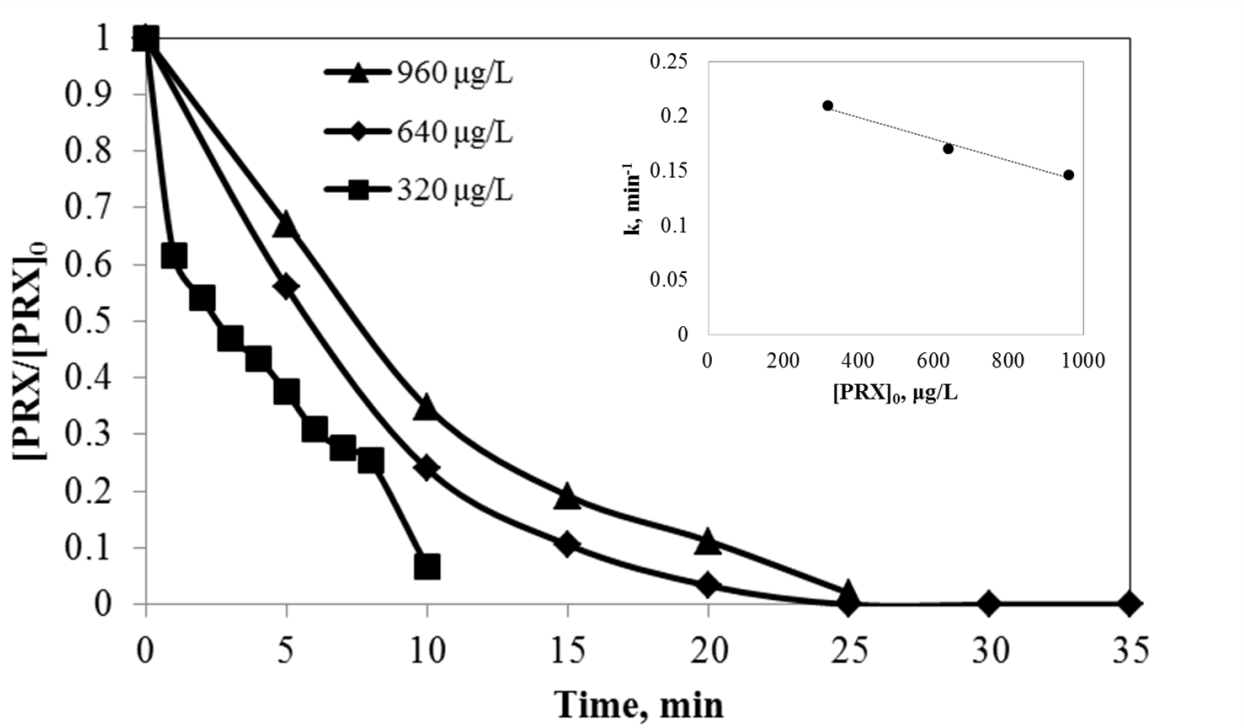

Figure 1

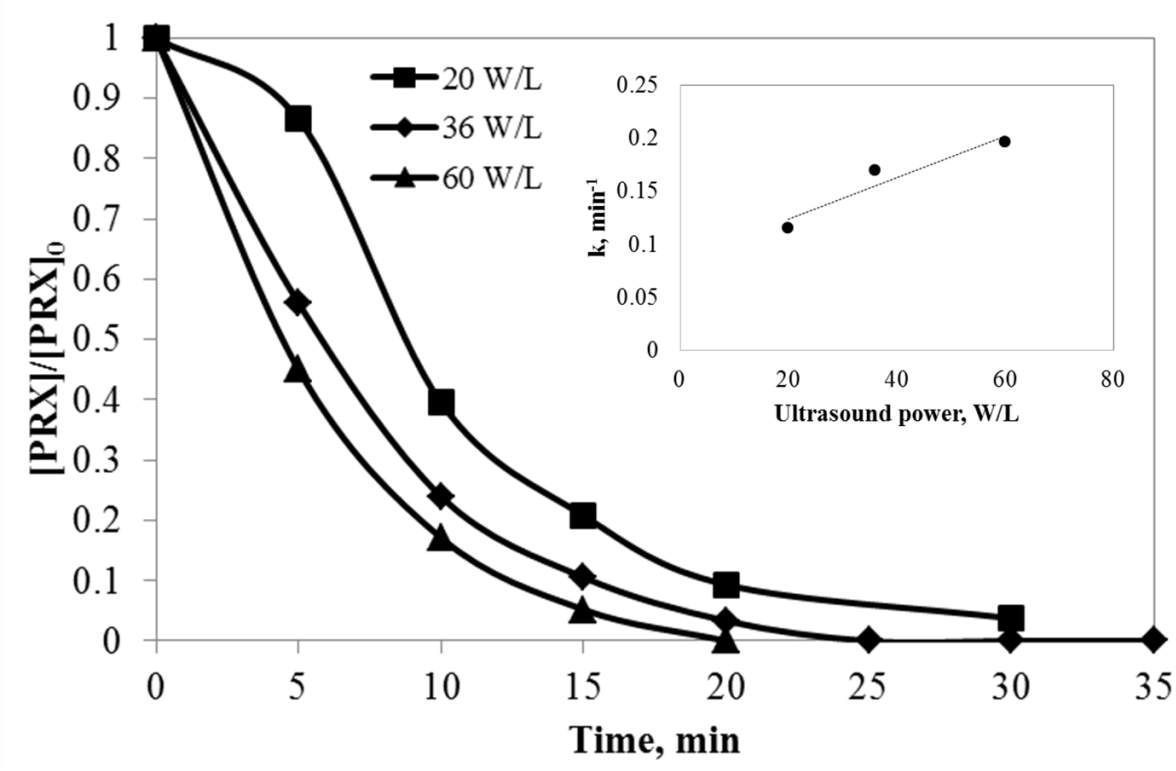

Figure 2

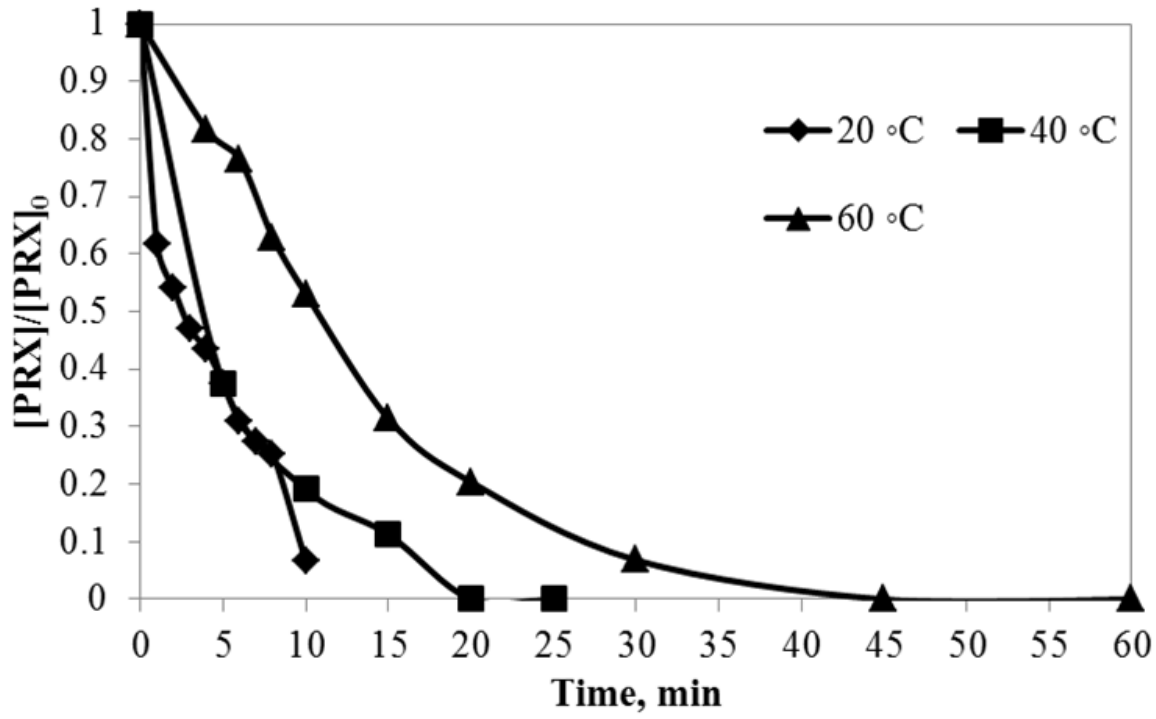

438

439 Figure 3

440

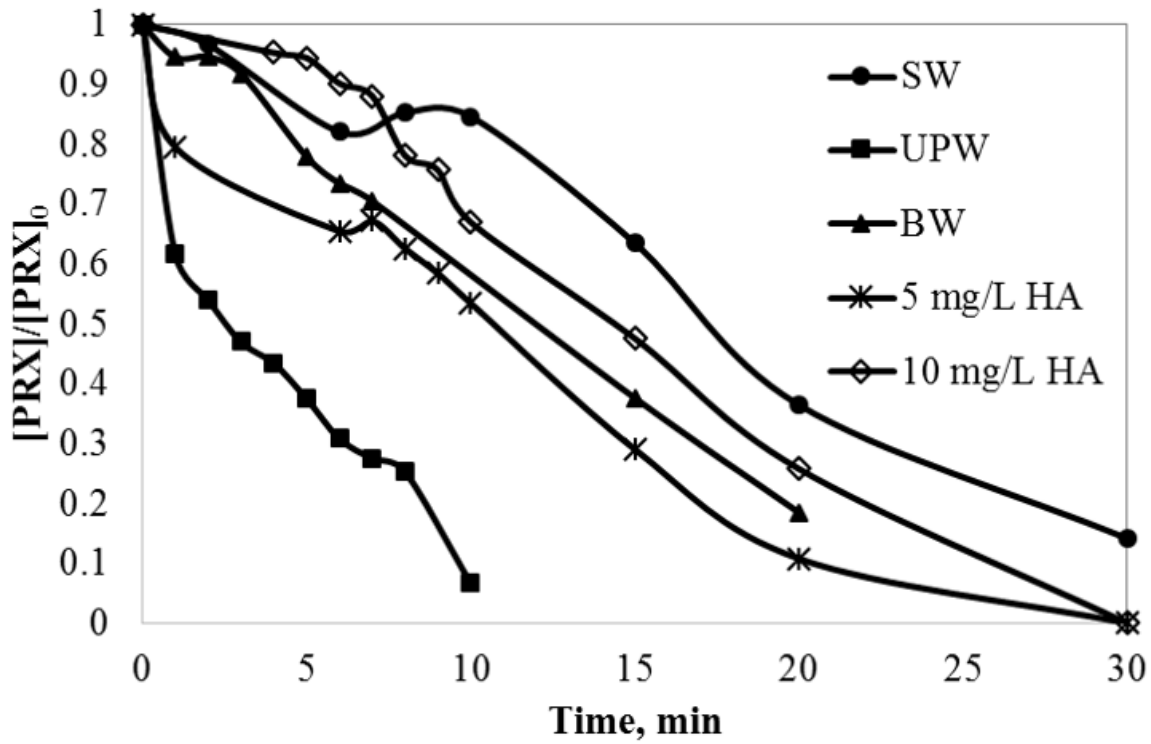

441

442 Figure 4

443

444

445

446

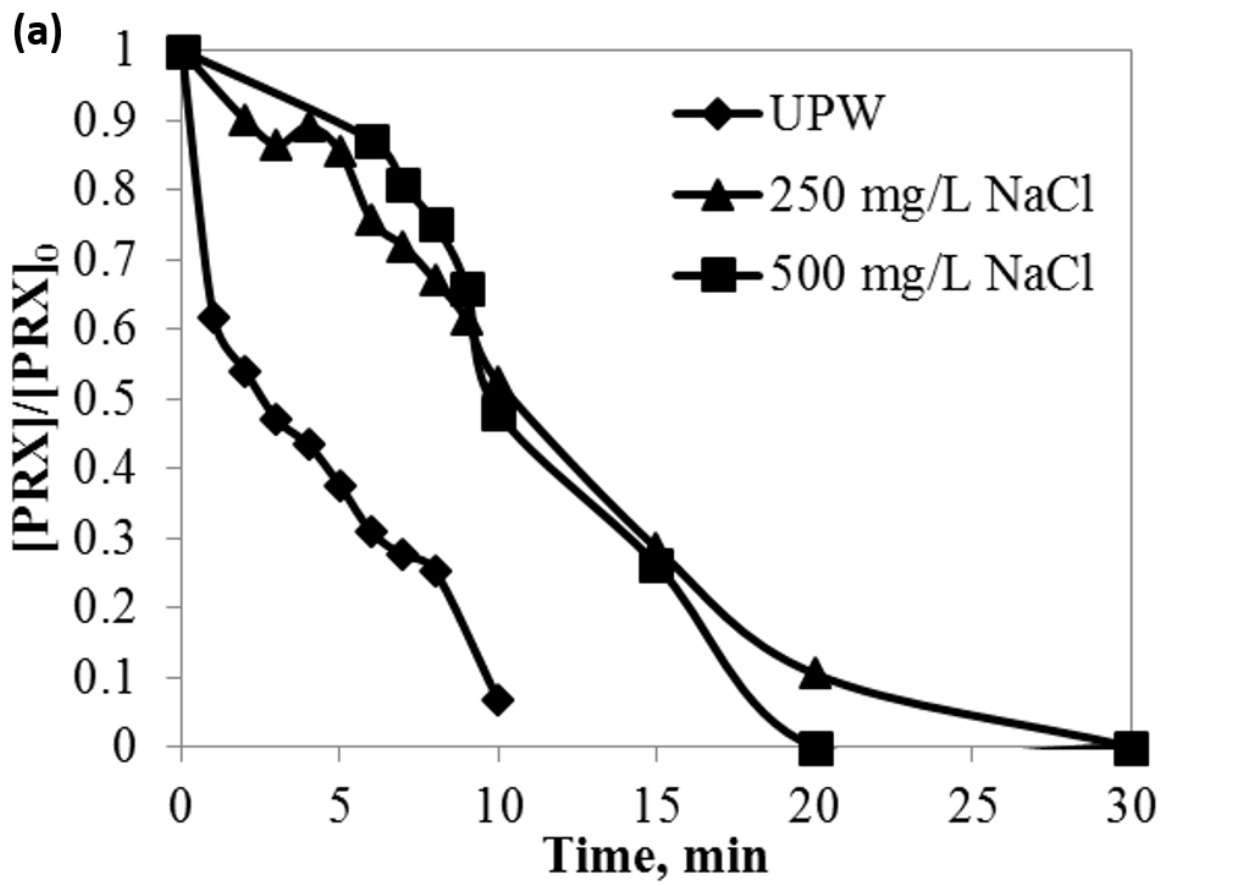
(a)
1
0.9
0.8
0.7
0.6
0.5
0.4
0.3
0.2
0.1
0
[PRX]/[PRX]0
0
5
10
15
20
25
30
Time, min
UPW
250 mg/L NaCl
500 mg/L NaCl

447

448

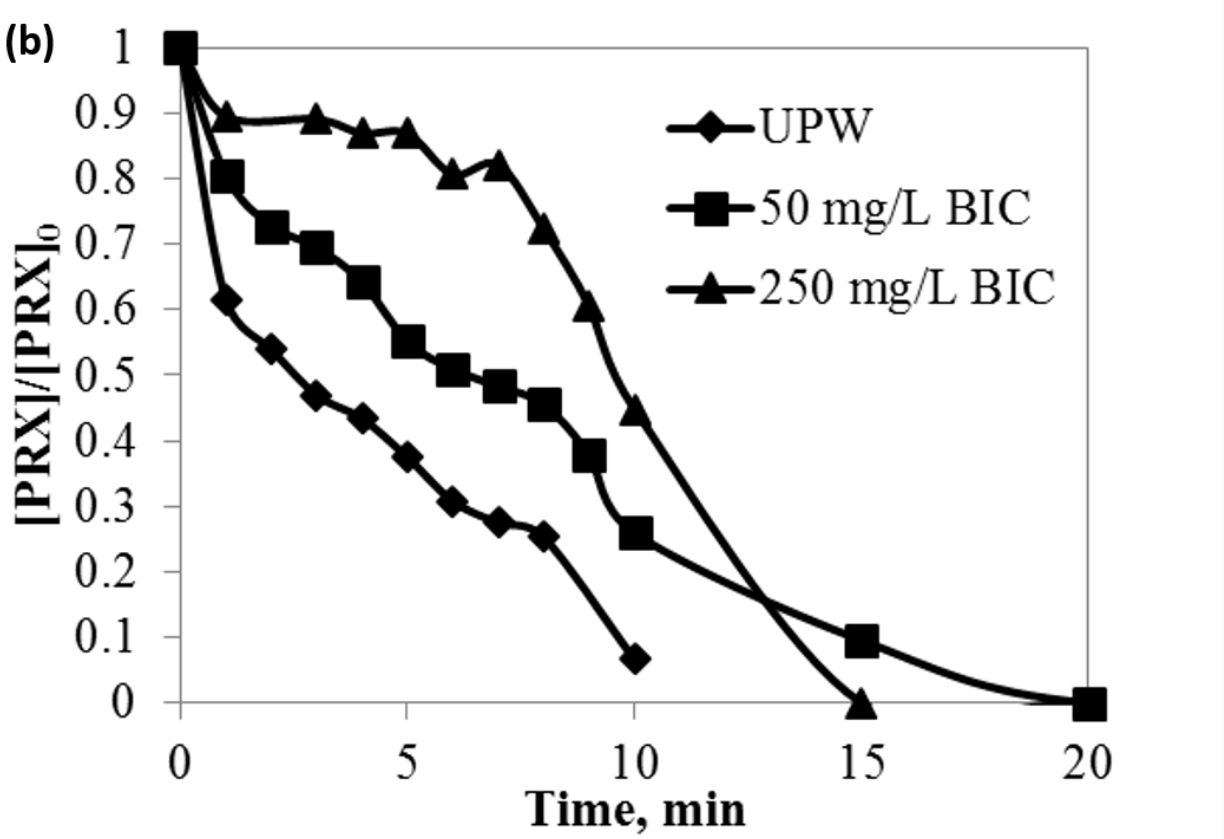

449

450 Figure 5

451

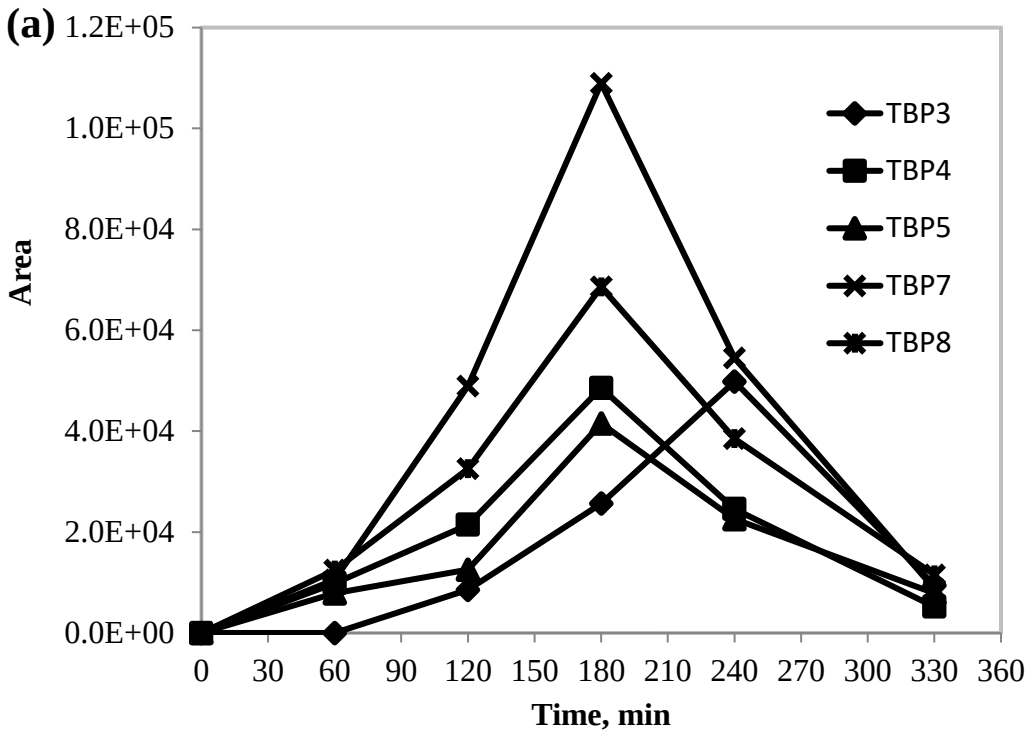

452

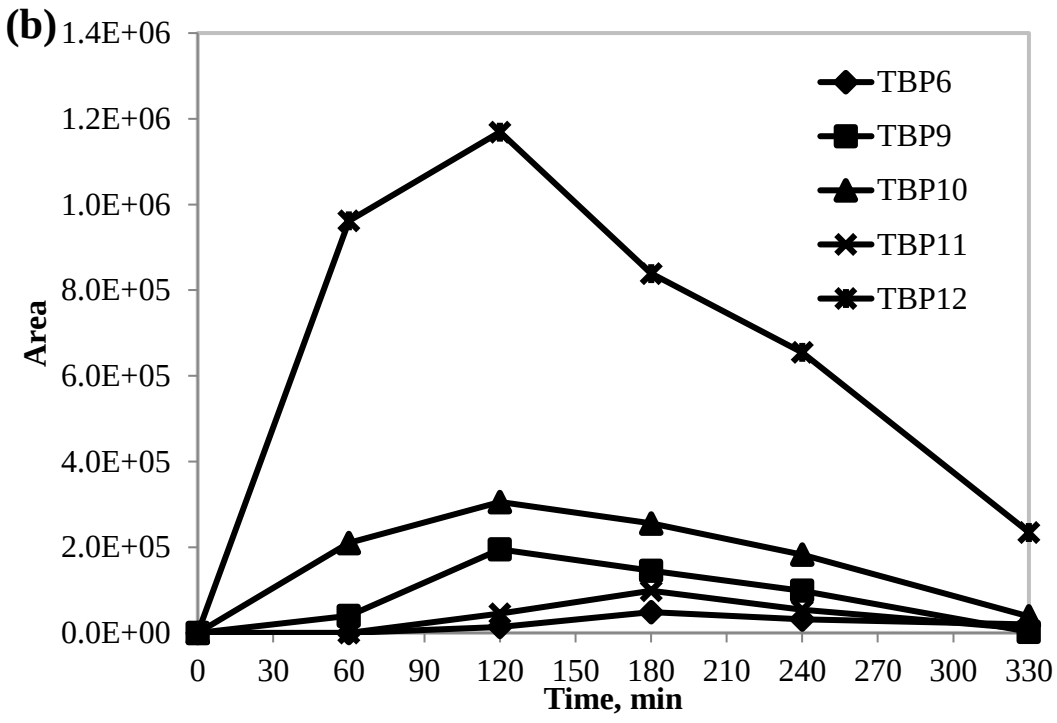

453

454 Figure 6

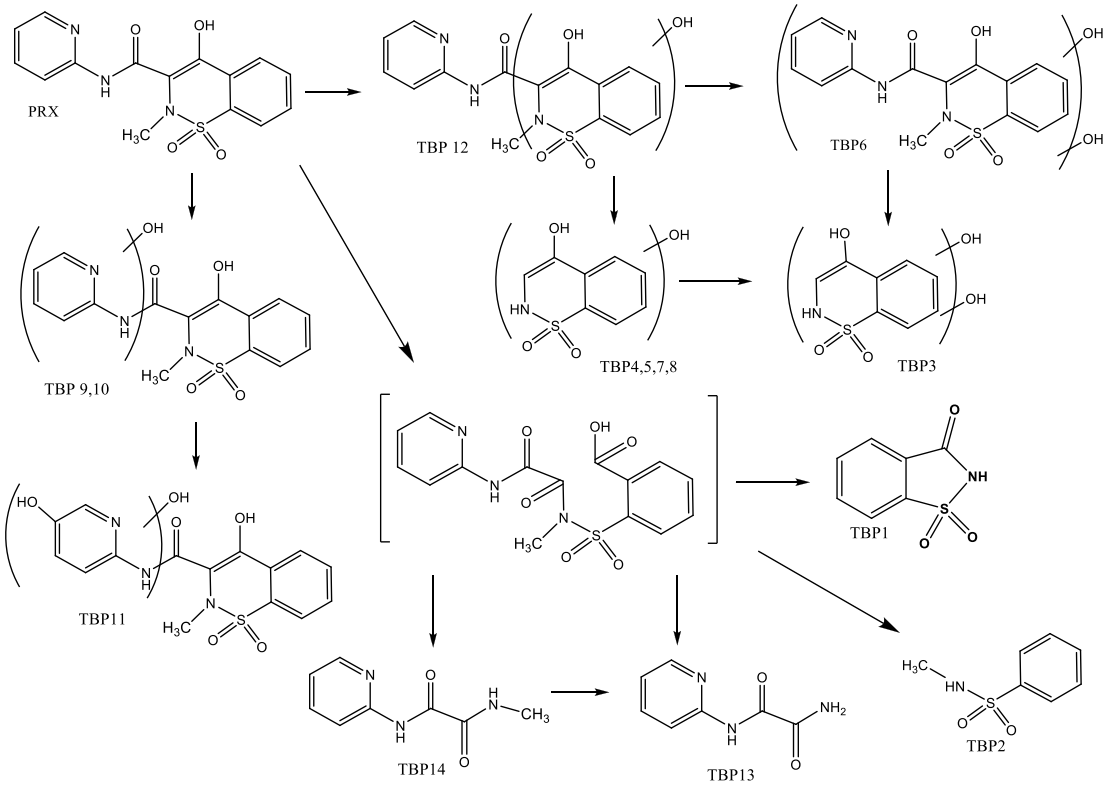
PRX
TBP 12
TBP6
TBP 9,10
TBP4,5,7,8
TBP3
TBP11
TBP1
TBP14
TBP13
TBP2

Figure 7